Deterministic-Stochastic Subspace Identification Method for Identification of Nonlinear Structures as Time-Varying Linear Systems

Babak Moaveni[1] and Eliyar Asgarieh[2]

ABSTRACT

This paper proposes the use of the deterministic-stochastic subspace identification (DSI) method, an input-output parametric linear system identification method, for characterization of nonlinear dynamic structural systems based on their time-varying amplitude-dependent instantaneous (i.e., based on short time-windows) modal parameters. Performance of the DSI method for estimation of instantaneous modal parameters of nonlinear systems is investigated using numerical as well as experimental data. In this study, DSI is used for extracting instantaneous modal parameters of single degree-of-freedom (SDOF) as well as 7-DOF systems with different hysteretic material behavior. Nonlinear responses of the SDOF and 7-DOF systems are simulated due to different seismic excitations using the OpenSees structural analysis software. Modal identification results are compared with those obtained using wavelet transform and the exact values. Effects of four input factors are studied on the variability of identified instantaneous modal parameters: (1) type of material nonlinearity, (2) level of nonlinearity, (3) input excitation, and (4) length of data windows used in the identification. The accuracy of the identified instantaneous modal parameters is evaluated along the response time history while varying the above mentioned input factors. Overall, DSI outperforms the wavelet transform for short-time/instantaneous modal identification of nonlinear structural systems and provides reasonably accurate results especially when the material hysteretic behavior is smooth such as the considered Giuffré-Menegotto-Pinto hysteretic model. Finally, DSI has been applied for short-time modal identification of a full-scale seven-story reinforced concrete shear wall structure based on its measured response to different seismic base excitations on a shake table. The identified instantaneous natural frequencies of the first vibration mode can accurately track the variation in the structure‟s effective stiffness along its response.

Keywords: Nonlinear system identification; instantaneous modal parameters; deterministic-stochastic subspace identification method.

[1] Corresponding author, Assistant Professor, Dept. of Civil and Environmental Engineering, Tufts University, Medford, Massachusetts 02155, USA; E-mail: babak.moaveni@tufts.edu

[2] Graduate student, Dept. of Civil and Environmental Engineering, Tufts University, Medford, Massachusetts 02155, USA; E-mail: eliyar.asgarieh@tufts.edu

1. Introduction

Nonlinear system/structural identification is defined as development of structural models (not necessarily in the form of a physics-based model) using dynamic measurements in the presence of nonlinearity. Kerschen et al. [1] classified the nonlinear system identification methods in the literature into the following seven categories: time-domain methods, frequency-domain methods, time-frequency methods, methods that by-pass nonlinearity using linearization, modal methods, black-box methods, and structural model updating methods. Some researchers have had success identifying hysteretic material behavior for civil structures (e.g., parameters of a Bouc-Wen model) using time-domain methods [2-4], time-frequency methods [5, 6], and use of unscented/extended Kalman filters for calibration of time-varying state-space models [7-9]; however, system identification of complex structures with many degrees of freedom (DOFs) would require estimating a large number of modeling parameters when numerical models are used. Methods based on time domain metrics require including a large number of data points from the response time history in the objective function and therefore, the optimization process can be computationally expensive or prohibitive. More importantly, these methods are usually very sensitive to measurement noise and modeling errors. To address these shortcomings, nonlinear system identification of large and complex structures can be performed by extracting low dimensional features such as time-varying instantaneous natural frequencies and mode shapes of few lower vibration modes, or nonlinear normal modes [10-12]. It is worth noting that nonlinear dynamic response of civil structures is usually dominated by their lower vibration modes. In addition, large-scale civil structures rarely experience highly nonlinear vibration phenomena such as bifurcation or chaos. This makes the characteristic of these structures as time-varying linear systems more realistic.

Several damage identification methods are based on the changes in dynamic characteristics of a system such as modal parameters that are considered as sensitive features to structural damage [13, 14]. Linear system identification methods have been successfully used by many researchers for experimental modal analysis of structures based on input-output measurements [15-17] as well as operational modal analysis based on output-only measurements [18-22] for the purpose of vibration-based structural health monitoring (SHM). However, these modal analyses methods are based on the assumption that measured data represent a linear dynamic response of the considered structure. Even though the modal analysis theory does not hold for nonlinear systems, it can be used as a tool to characterize specific types of nonlinear dynamic systems such as real-world civil structures with material nonlinearity based on their instantaneous/short-time modal parameters along the nonlinear response time history. These instantaneous modal parameters correspond to an equivalent linear system with stiffness equal to tangent stiffness of the nonlinear system at considered time instant. In structural and earthquake engineering

communities, computation of nonlinear dynamic response of civil structures due to moderate to large amplitude excitations (common in design, response prediction, and reliability of structures) is performed through linearization of nonlinear stiffness matrix at each time instant (i.e., frozen configuration). This study proposes to use a linear system identification method to estimate the instantaneous modal parameters of a nonlinear structure. The identified instantaneous modal parameters can be used to estimate the instantaneous stiffness of elements (or substructures) - through solving an inverse problem (e.g., finite element model updating) - corresponding to the tangent stiffness matrix of the considered structure. Among linear system identification methods, the data-driven subspace identification methods (SSI-Data) [23, 24] is the most reliable output-only operational modal analysis methods while the deterministic-stochastic subspace identification methods (DSI) is the most accurate input-output experimental modal analysis method [25-27]. The DSI method provides accurate results even when applied to short segments of data. This paper investigates the performance of the DSI method for short-time (instantaneous) system identification of nonlinear systems when subjected to non-stationary seismic base excitations. Although DSI is one of the most common methods for experimental modal analysis, to the knowledge of authors, there is no previous application of DSI for short-time modal identification.

In the literature, several time-frequency identification methods such as short-time Fourier transform (STFT), wavelet transform (WT), Hilbert-Huang transform (HHT), and proper orthogonal decomposition (POD) have been proposed for short-time modal identification of nonlinear structural systems. STFT is the simplest approach for tracking changes in the instantaneous natural frequencies and mode shapes along the response time history. This method uses the Fourier transform of short windows of data in a signal. The main shortcoming of this method is the low resolution of the identified natural frequencies when the time windows become smaller (i.e., compensation between time and frequency resolutions due to Heisenberg uncertainty principle). WT has been used in the context of structural health monitoring to extract instantaneous natural frequencies and damping ratios of structures based on their free vibration response [28, 29]. Methods to improve the accuracy of WT for structural identification have been proposed by several researchers [30-34]. It should be noted that similar to other time-frequency methods, WT also suffers from the compensation between time and frequency resolutions. Spanos [35] has used WT for estimation of instantaneous frequencies of time-varying systems. Hilbert transform has been applied for identification of linear and nonlinear systems [36-39]. Since Hilbert transform can only identify one frequency at a time, it is more suitable for single degree-of-freedom (SDOF) systems. Hilbert-Huang method has been implemented for identification of multi degree-of-freedom (MDOF) systems [40-43]. POD has also been used by many researchers for modal analysis as well as finite element model updating of nonlinear systems [44-47]. The above mentioned methods provide good estimates of instantaneous modal parameters when applied to the nonlinear response of systems subjected

to broadband and stationary inputs. However, the identification errors for these methods increase as the input excitation signals become more narrow-band and non-stationary. It is also worth noting that several methods exist in the literature for time-varying linear system identification such as time-varying auto-regressive with exogenous input (TV-ARX) [48, 49], time-varying auto-regressive moving average (TV-ARMA) [50], and some derivatives of TV-ARMA [51, 52]. These methods are extensions of the classical prediction error methods (PEMs).

In this study, performance of the DSI method for short-time (instantaneous) system identification of nonlinear systems when subjected to non-stationary seismic base excitations is investigated. Accuracy of this method is compared to that of the wavelet transform method when applied for identification of SDOF as well as 7-DOF systems with different material hysteretic behavior. It is worth noting that other sources of nonlinearity such as friction or impact are not considered in the numerical models because these types of nonlinearities cannot be properly linearized. Therefore, this is one of the shortcomings of the proposed nonlinear structural identification method based on instantaneous modal parameters. Effects of several input factors on the accuracy of system identification results are studied. The considered input factors are: (1) type of material nonlinearity (i.e., material hysteretic behavior), (2) level of nonlinearity, (3) input excitation, and (4) length of the "short-time" data windows used in the identification. Finally, DSI has been used for short-time system identification of a full-scale seven-story reinforced concrete shear wall structure based on its measured nonlinear response to different seismic base excitations on a shake table.

This paper is organized in the following order. Section 2 of the paper describes the input factors and their considered levels. Section 3 reviews the numerical simulation of nonlinear dynamic response for the SDOF and 7-DOF systems with different material hysteretic models and for different input excitations. The system identification process and the obtained results are presented in Section 4. Section 5 provides an uncertainty analysis of the system identification results in the view of input factors variability. Section 6 reports the short-time system identification results of the full-scale seven-story shear wall using DSI. Finally, the concluding remarks are provided in Section 7.

2. Input Factors Considered in the Numerical Study

As previously mentioned, the variability of system identification results (instantaneous natural frequencies and damping ratios) obtained using the DSI are studied due to variability of four input factors. Each of the input factors is considered at two levels. The input factors and their considered ranges are selected based on the authors" previous experience in system identification of civil structures. Considering a full factorial design of experiment (i.e., all combination of input factor levels are considered), $2\times2\times2\times2=16$ sets of system identifications with varying input factors are performed for each type of

system (i.e., SDOF and 7-DOF). Each set of system identification results are obtained by the application of DSI and WT along the response time history resulting in 1,280 (= 16 x 2 systems x 40 time instances) identifications using DSI and 640 (= 8 x 2 systems x 40 time instances) identifications using WT. Table 1 reports the input factors and their considered levels. More details about the input factors are given in the following subsections.

2.1. Type of Material Nonlinearity (M)

Variability of this input factor allows studying the sensitivity of short-time system identification results to the choice of material hysteretic model. Two types of material models commonly used for steel are considered in this study, namely (1) bilinear, and (2) Giuffré-Menegotto-Pinto hysteretic models. A strain hardening ratio of 0.1 is considered for both of the material types while the yield strength is assigned based on the level of nonlinearity. Figure 1 shows the force-displacement hysteretic behavior of these two material models with a strength reduction factor of R = 4 when subjected to a considered Northridge earthquake record. It should be noted that more complicated material models that include stiffness and/or strength degradation are not considered in this study in order to avoid extra sources of variability/uncertainty and limit the number of input factors.

2.2. Level of Nonlinearity (R)

With increasing level of response nonlinearity, the estimation error in system identification results using linear methods are expected to increase. Variability of this input factor allows evaluating the accuracy of DSI results when applied to dynamic data of increasing nonlinearity. The level of response nonlinearity is defined as the strength reduction factor (R). For each of the material models, two different levels of nonlinearity are considered: R = 4 and R = 6. For an input excitation, the R factor is defined as the ratio of maximum force produced in an equivalent linear system to the yielding strength. The strength reduction factor is assigned to each material model by adjusting its yield strength. Figure 2(a) compares the response time histories of two SDOF systems with Giuffré-Menegotto-Pinto material models and R factors of 4 and 6 when subjected to the considered Northridge earthquake record while Figure 2(b) compares the force displacement hysteretic response of two SDOF systems with bilinear material models and R factors of 4 and 6 when subjected to a considered Imperial Valley earthquake record. It can be observed that by increasing the strength reduction factor, the response becomes more nonlinear.

2.3. Input Excitation (I)

Various characteristics of a ground motion such as its frequency content, pulsing sequence, and duration can have significant effects on the nonlinear response of structures. In this study, two earthquake

records with different frequency contents and durations are used as the input excitations. The first excitation is the longitudinal component of the 1994 Northridge earthquake (M_w = 6.7) recorded at the Oxnard Boulevard station in Woodland Hills, which is a near field record with the closest distance of 16.7 km to the fault. The second excitation is selected as the longitudinal component of the 1979 Imperial Valley earthquake (M_w = 6.5) recorded at the Delta station, which is a far field record with closest distance to the fault of 43.6 km. The time history and Fourier amplitude spectra (FAS) of these excitations are shown in Figure 3. It should be noted that both of these records are re-sampled to have a sampling rate of 256 Hz.

2.4. Length of Data Time-Windows Used in Identification (L)

The accuracy of most system identification methods depend on the amount of data used in the identification process [25]. In this study, DSI is applied to input-output data windows of two different lengths: 1-second and 2-second time windows corresponding to 256 and 512 data points, respectively (sampling frequency is 256 Hz). A short-time system identification is performed every one second along the response time history when the numerical models are subjected to the Northridge earthquake, i.e., there is a 50% overlap between consecutive 2-second windows of data. However, in order to limit the number of system identifications during the longer Imperial Valley earthquake, short-time system identifications are performed every two seconds along the response time histories, i.e., there is a no overlap between consecutive data windows when this earthquake is applied.

3. Numerical Simulations

Nonlinear response of SDOF and 7-DOF dynamic systems corresponding to different combinations of input factors are simulated using the object-oriented software framework OpenSees for advanced modeling and response simulations of structural and geotechnical systems [53]. Simple truss elements are used to model the SDOF systems while the 7-DOF systems are modeled with beam-column elements with lumped translational masses at FE model nodes. In the 7-DOF systems, rotational DOFs at the nodes are restrained so the models can represent simplified seven-story shear buildings. The nonlinearity for each of the 7-DOF models is applied at the first element only (bottom story) with concentrated nonlinear behavior at the element ends. The material type of steel01 in OpenSees is used for the bilinear material model and the material type of steel02 is used to model the Giuffré-Menegotto-Pinto material behavior. The Newmark-Beta method is used as the time integration method for all models. The natural frequency of the underlying linear SDOF systems (corresponding to the initial stiffness) is 2 Hz and the damping ratio is assigned as 2%. For the 7-DOF systems, viscous Rayleigh damping is assigned with 2% damping ratios at

frequencies 2 Hz and 10 Hz. Table 2 shows the natural frequencies and damping ratios of the underlying linear 7-DOF system.

4. System Identification based on Numerical Data

DSI and WT methods have been applied for short-time/instantaneous modal identification of SDOF and 7-DOF structural models with different considered input factors and along their response time histories. In the section, these two system identification methods are briefly reviewed and their modal identification results are presented and discussed.

4.1. Deterministic-Stochastic Subspace Identification (DSI)

The DSI is a parametric linear system identification method that determines the system model in state-space based on the input-output measurements directly [23]. This method is robust in view of the input disturbance and measurement noise as both terms are explicitly considered in its formulation. It involves numerical techniques such as QR factorization, singular value decomposition and least squares. In the current application of the DSI, a Hankel matrix is formed using the input-output data with 42 block-rows (2 rows per block) for each SDOF system and with 14 block-rows (8 rows in each block) for each 7-DOF system when the window length of 1 second is used. In the case of using 2-second data windows, the corresponding Hankel matrices have 80 block-rows for the SDOF systems and 28 block-rows for the 7-DOF systems. Stabilization diagrams have been used to select the model order and choose the physical (as opposed to numerical/spurious) vibration modes.

4.2. Wavelet Transform (WT)

WT method for system identification is a non-parametric and output-only identification method. In this study, complex Morlet wavelet is used as the basis function. The basis function in a Morlet wavelet is a Gaussian windowed harmonic function and there is a direct relation between the scale values and the dominant frequency of the wavelet. The selected complex Morlet wavelet has a bandwidth parameter of 2 and a central frequency of 1 Hz ($f_b = 2, f_c = 1$). These parameters are selected based on the characteristics of the nonlinear systems considered in this study [33]. In the application of WT for modal identification, the instantaneous natural frequency of a system is identified as the frequency that corresponds to the peak of wavelet spectrum at that time instant. Figure 4 shows a sample wavelet spectrum of the nonlinear response of a SDOF system with bilinear material nonlinearity and R = 6 when subjected to the Northridge earthquake and at the time instant t = 17 s. It is worth noting that when working with MDOF systems, the WT is known to be a suboptimal choice with respect to other time-frequency transforms because it is essentially a time-scale representation. However, from the practical point of view, in most

applications of WT for identification of civil structures, WT is used to track the instantaneous natural frequency of the predominant vibration mode.

4.3. System Identification Results

The DSI and WT methods have been used for modal identification of the considered SDOF and 7-DOF systems for 16 different combinations of input factors in the case of DSI and 8 in the case of WT (data length is not considered as a source of variability for WT). For each combination, short-time system identifications are performed along the time history of nonlinear dynamic response (every one second for the Northridge earthquake and every two second for the Imperial Valley earthquake). For the 7-DOF system, the DSI is used for estimation of instantaneous natural frequencies and damping ratios of the first three vibration modes while the WT is used for estimating the natural frequencies of the first vibration mode only, as higher modes could not be identified by WT. The identified natural frequencies at each time window are compared with their average exact counterparts that are obtained from the nonlinear FE model. The identified frequencies using DSI correspond to an effective linearized system that represents the nonlinear system over the considered window length and therefore should be compared to the average of exact natural frequencies over all time instants along the window length. The exact instantaneous natural frequencies of a nonlinear system can be obtained at any time instant (the time resolution in this study is $\Delta t = 1/256$ s) by eigenanalysis of the tangent stiffness matrix. Note that the average of instantaneous natural frequencies is different than the natural frequency obtained from eigenanalysis of the average tangent stiffness matrix. The identified damping ratios correspond to the total energy dissipation mechanism including the viscous as well as hysteretic behavior. Therefore, the identified damping values can also provide a measure of response nonlinearity. Higher instantaneous damping ratios indicate higher levels of nonlinear hysteretic behavior.

Figure 5 shows the identified natural frequencies and damping ratios of a linear SDOF system along its response time history (every 1 second) when subjected to the Northridge earthquake using DSI and WT methods together with the exact values shown as solid lines. It can be observed that the DSI method can accurately identify the natural frequency and damping ratio of the SDOF system using short time windows while the estimates using WT method have larger errors. Figure 6 shows the identified modal parameters of a linear 7-DOF system along its response time history when subjected to the Northridge earthquake using DSI. Modal parameters of all seven modes are accurately identified. The identified damping ratios have larger estimation errors than the identified natural frequencies; and the estimation errors for both the natural frequencies and damping ratios increase for the higher modes. The WT method is only reliable for identification of the first natural frequencies, which are also shown on Figure 6.

Figures 7-10 show four samples of short-time system identification results from the total 32 identification cases (16 combinations of input factors for two types of systems). Figure 7 shows the identified modal parameters of a SDOF system with bilinear material nonlinearity (M = bilinear) and R factor of 6 (R = 6) along the nonlinear dynamic response time history due to the Northridge earthquake base excitation (I = Northridge) for data windows of 2 seconds long (L = 2). Figure 8 plots the short-time modal identification results for a SDOF with the following input factors: M = Pinto (short for Giuffré-Menegotto-Pinto), R = 6, I = Imperial Valley, and L = 1. Figure 9 presents the identified modal parameters of a 7-DOF system (only the first three modes) with the choice of input factors as M = bilinear, R = 4, I = Imperial Valley, and L = 2 while Figure 10 corresponds to M = Pinto, R = 4, I = Northridge, and L = 1. In the case of the 7-DOF systems, DSI could identify the first three vibration modes while the WT could only estimate the first vibration mode. From Figures 7-10 and the other 28 short-time system identification plots not shown here, it is observed that:

(1) The level of response nonlinearity can be tracked through identified instantaneous natural frequencies and damping ratio using DSI.
(2) Modal parameters obtained using DSI are consistently more accurate than those obtained using WT.
(3) Estimated modal parameters of the first mode of the 7-DOF systems are more accurate than those of the SDOF systems with similar input factors. This is most likely due to the fact that in system identification of the 7-DOF systems, seven channels of output measurements are used in each block row of the data Hankel matrix as compared to one output channel for the SDOF systems.
(4) DSI results are more accurate (closer to the average exact natural frequencies) for nonlinear systems with smooth hysteretic behavior (Pinto) than those with bilinear hysteretic behavior.
(5) Estimation errors of the identified modal parameters of the 7-DOF systems increase for higher modes.
(6) The identified effective damping ratios appear to be more sensitive to the level of response nonlinearity than the corresponding instantaneous natural frequencies.

5. Uncertainty Analysis of System Identification Results Based on Numerical Data

In this section, effects of different input factors on the short-time system identification results are studied. In Section 5.1, two error metrics are defined and the accuracy of system identification results is studied based on these two metrics. The influence of each input factor on the variability of estimation errors is quantified in Section 5.2 using an effect screening method.

5.1. Mean and Maximum Estimation Errors

In this study, two error metrics are used for quantifying the accuracy of system identification results. These metrics are defined as the mean estimation error and maximum estimation error. Estimation error

of an identified natural frequency refers to absolute value of the difference between identified natural frequency and the corresponding exact value (averaged over the length of time window). Figure 11 shows a sample of estimation error time history for the identified natural frequencies of a SDOF system with M = Pinto, R = 6, I = Northridge, and L = 2 using DSI and WT methods. It is observed that the estimation errors of the DSI results are significantly smaller than those from the WT.

The mean estimation error and maximum estimation error are defined as the mean and maximum of the estimation error time histories, respectively, computed over the strong motion part of the considered earthquakes. The strong motion part of the Northridge earthquake, corresponding to higher level of response nonlinearities, is considered between 2 and 20 s while the strong motion part of the Imperial Valley earthquake is considered between 5 and 40 s. Tables 3 and 4 report the mean and maximum estimation errors of the DSI and WT methods for the SDOF and 7-DOF systems, respectively. From these tables, it is found that:

(1) The estimation errors of DSI results are systematically smaller than those of WT results. This is consistent with observations from Figures 7-11.
(2) The system identification results using WT are very sensitive to the input excitation. This is due to the fact that WT is an output-only method and does not use any information about the input excitation in the identification process.
(3) In general, the DSI estimation errors for models with bilinear material behavior are larger than those for the model with Pinto material behavior.
(4) Use of larger data windows improves the DSI results for the 7-DOF systems, especially the first vibration mode, while this input factor does not show a clear effect on the identified modal frequencies of the SDOF systems.

The standard deviation of the mean and maximum estimation errors of DSI results for the SDOF and 7-DOF systems over the 16 combinations of input factors are reported in Table 5. From this table, it is seen that the maximum estimation errors exhibit much larger variability than the mean estimation errors.

5.2. Effect Screening

To quantify the influence of each input factors to the total variability of the mean and maximum estimation errors (Table 5), an analysis-of-variance (ANOVA) [54] is performed. The theoretical foundation of ANOVA is that the total variance of the output features (estimation errors) can be decomposed into a sum of partial variances, each representing the effect of varying an individual factor independently from the others. Contribution of each partial variance to the total variance is estimated by the coefficient-of-determination R^2 value. The input factor with the largest R^2 value for an output feature

has the most contribution to the variability of that output feature. In this study, ANOVA is applied to 16 sets of output features (i.e., mean and maximum estimation errors for natural frequencies of modes 1-3). Figure 12 shows the R^2 values of the mean and maximum estimation errors of the identified natural frequencies for SDOF and 7-DOF systems. These R^2 values are scaled such that their sum over all factors equates 100%. From Figure 12, the following observations can be made based on the considered input factors and their variation levels.

(1) In modal identification of SDOF systems, the level of nonlinearity has the most influence on mean estimation error while the type of nonlinearity is the most important factor for maximum estimation error.
(2) In modal identification of 7-DOF systems, the type of material nonlinearity and the length of data windows have the most contributions to the total variability of both mean and maximum estimation errors of the first mode natural frequency.
(3) The type of input excitation has larger effects on the variability of estimation errors for the higher vibration modes (modes 2 and 3).

6. System Identification Based on Experimental Data

This section is focused on the application of DSI for short-time system identification of a full-scale seven-story shear wall structure, which was tested on a shake table. Section 6.1 briefly describes the test structure and the dynamic tests performed. The short-time system identification results of this specimen when subjected to three historical earthquake base excitations are presented in Section 6.2.

6.1. Test Structure and Dynamic Tests Performed

The test structure is a full-scale seven-story reinforced concrete shear wall, consisting of a main wall (web wall), a back wall (flange wall) perpendicular to the main wall for transversal stability, a concrete slab at each floor level, an auxiliary post-tensioned column to provide torsional stability, and four gravity columns to transfer the weight of the slabs to the shake table. Figure 13 shows the test structure mounted on the University of California San Diego (UCSD)-NEES shake table. More details about the test structure can be found in [55]. The test structure was instrumented with a dense array of accelerometers, strain gages, potentiometers, and linear variable displacement transducers, all sampling data simultaneously using a nine-node distributed data acquisition system. The structure has been excited by four historical earthquakes with increasing intensity. In this study, measured response data from seven longitudinal acceleration channels at the floor levels and the input acceleration measured on top of the

shake table are used for short-time system identification of the test structure during the seismic base excitations.

The structure was damaged progressively through four earthquake ground motions. The four earthquake records applied to the test structure were: (1) longitudinal component of the 1971 San Fernando earthquake (M_w = 6.6) recorded at the Van Nuys station (EQ1), (2) transversal component of the 1971 San Fernando earthquake recorded at the Van Nuys station (EQ2), (3) longitudinal component of the 1994 Northridge earthquake (M_w = 6.7) recorded at the Oxnard Boulevard station in Woodland Hill (EQ3), and (4) 360 degree component of the 1994 Northridge earthquake recorded at the Sylmar station (EQ4). DSI has been applied to the measured input-output data from the last three earthquakes for short-time system identification. Figure 14 shows the acceleration time history of input base excitations measured on the shake table for EQ2, EQ3, and EQ4, together with the hysteretic curve of base moment versus roof displacement (computed from numerical integration of measured roof acceleration) for each earthquake. The base moment was estimated using the floor accelerations and their contributory masses. It is worth noting that for the considered dynamic tests, base moment versus roof displacement curves provide more clear hysteretic behavior of the structure than other types of hysteretic curves such as base shear versus roof displacement [55]. From Figure 14, it can be seen that EQ2 and EQ3 result in similar levels of response nonlinearity in the shear wall while the nonlinearity in the response due to EQ4 is significantly larger. More details about the instrumentation and dynamic testing of the test structure can be found in [26]. It is worth noting that the during the shake-table experiment of the 7-story reinforced concrete wall, significant stiffness degradation was observed while the strength reduction was negligible. However, in the numerical examples, the considered nonlinear material models (bilinear and Pinto) do not include any stiffness and strength degradations (progressive damage) for simplicity. Stiffness and strength degradation can be considered in more complex material models such as Bouc-Wen models, which can take from 5 up to 13 parameters depending on whether stiffness degradation, strength degradation and pinching behavior are considered in the model or not [56].

6.2. System Identification Results

DSI is applied for short-time system identification of the test structure based on its measured test data during the three considered earthquake base excitations. The input excitation and the response acceleration of the shear wall were sampled at 240 Hz. Similar to the numerical examples, two different lengths of data windows (1 and 2 seconds) are considered for estimation of instantaneous modal parameters at every one second along the response time history (i.e., 50% overlap between consecutive 2-second windows). In the application of DSI, Hankel matrices of size (26 x 8) x 215 and (52 x 8) x 422 are

formed based on 1 or 2 seconds of data, respectively. For each short-time system identification, the model order is selected using a stabilization diagram.

Figure 15(a) shows the time histories of the first mode instantaneous natural frequency of the test structure identified using 1- and 2-second windows during the three considered earthquake base excitation tests. Figure 15(b) plots the square root of an effective global stiffness estimate of the structure during the base excitation time histories. The effective global stiffness of the test structure at each time window is estimated as the secant stiffness of base moment versus roof displacement hysteretic curve during that time window (1- and 2-second). The secant stiffness is computed as the slope of straight line connecting the extreme displacement points on the hysteretic curves. From this figure, it is observed that:

(1) The identified instantaneous natural frequencies during all three earthquakes decrease drastically during the first part (highest energy part) of the strong motion and then will increase slightly as the response amplitude (i.e., level of nonlinearity) becomes smaller toward the end of earthquake. Note that the instantaneous natural frequency at the end of each earthquake is significantly smaller than that at the beginning of earthquake. This corresponds to the stiffness degradation in the test structure during each seismic event. However, the authors would like to emphasize that the stiffness degradation is usually not correlated with the strength degradation in the structure [57].
(2) Use of 2-second time windows for instantaneous modal identification provides a smaller number of missed identifications and outliers.
(3) The identified instantaneous natural frequencies match well the trend of the square root of effective global stiffness estimates. It is expected that accurate estimates of instantaneous modal parameters can be used for characterizing the hysteretic behavior of the structure at element/substructure levels. This is the topic of ongoing research by the authors.

Table 6 reports the first mode natural frequencies identified based on low-amplitude ambient vibration and 0.03 g root mean square (RMS) white noise base excitation tests performed before and after each earthquake test [26]. It should be noted that during the period between EQ3 and EQ4, the test structure was slightly reinforced and therefore the low-amplitude modal identification results from after EQ3 and before EQ4 are not the same. The natural frequencies identified from these low-amplitude dynamic tests are also shown in Figure 15(a). The instantaneous natural frequencies at the beginning and end of each earthquake are between the corresponding natural frequencies from ambient vibration and white noise tests, respectively. This is due to the fact that the response amplitude of the test structure at the beginning and end of considered earthquakes are bounded between the response due to ambient vibration and white noise base excitation tests. It can also be seen that in general, the instantaneous natural frequencies at the beginning of each earthquake are closer to the corresponding natural

frequencies identified based on the ambient vibration test data performed before the earthquake (except for EQ4) while the instantaneous natural frequencies at the end of each earthquake are closer to those identified based on white noise test data performed after the earthquake. This may be explained by the fact that the first few low-amplitude cycles of the ground motion cannot open the existing cracks in the test structure (due to friction) while these cracks will open due to the same level of input excitations at the end of the earthquake (after the structure is subjected to the strong motion part).

7. Conclusions

In this study, performance of the deterministic-stochastic subspace identification (DSI) method for instantaneous modal analysis of nonlinear dynamic systems is evaluated based on numerical as well as experimental data. In the numerical study, system identification results of nonlinear SDOF and 7-DOF systems obtained from DSI are compared to those from wavelet transform (WT) method and the exact values from finite element analysis. Accuracy of system identification results is investigated due to variability of four input factors: type of material nonlinearity, level of nonlinearity, input excitation, and length of data windows used in the identification. The contribution of each input factor to the total variability of two estimation error metrics is quantified through analysis-of-variance, an effect screening method. Based on this numerical uncertainty analysis study, the following observations are made.

(1) The response nonlinearity and its intensity can be tracked through identified instantaneous natural frequencies and damping ratio using DSI.
(2) The identified effective damping ratios appear to be more sensitive to structural response nonlinearity than the instantaneous natural frequencies. However, the damping ratios in general have a larger estimation uncertainty than the natural frequencies.
(3) Modal parameters obtained using DSI are consistently more accurate than those obtained using WT.
(4) The system identification results using WT are very sensitive to the input excitation. This is due to the fact that WT does not use any information about the input excitation in the identification process and therefore, its estimation error increases as the input excitation becomes more nonstationary.
(5) Estimation errors of the identified modal parameters increase for the higher modes.
(6) The type of material nonlinearity has a significant effect on the accuracy of system identification results. The identification results for nonlinear system with Giuffré-Menegotto-Pinto hysteretic models are closer to the exact values than those with bilinear hysteretic models.
(7) Use of larger data windows improves the DSI identification results of the 7-DOF systems, especially for the first vibration mode, while this input factor does not show a clear effect on identified natural frequency of the SDOF systems.

DSI is also used for short-time system identification of a full-scale seven-story shear wall structure when subjected to seismic base excitation through a shake table. The structure was damaged progressively through four historical earthquake ground motions. Measured response data from seven longitudinal acceleration channels at the floor levels and the input acceleration measured on top of the shake table were used for short-time system identification of the test structure during three seismic tests. The following observations are made from the system identification results of this test structure.

(1) The identified instantaneous natural frequencies during the considered three earthquakes decrease drastically during the first part (with highest energy) of the strong motion and then will increase slightly as the response amplitude (i.e., level of nonlinearity) becomes smaller at the end of earthquake.
(2) The instantaneous natural frequency at the end of each earthquake is significantly smaller than that at the beginning of the earthquake. This corresponds to the stiffness degradation in the test structure during each seismic event. However, the authors would like to emphasize that the stiffness degradation is usually not correlated with the strength degradation in the structure.
(3) The identified instantaneous natural frequencies match the trend of square root effective global stiffness estimate of the structure obtained from base moment versus roof displacement hysteretic curves.
(4) The instantaneous natural frequencies at the beginning and end of each earthquake are bounded between the corresponding natural frequencies from ambient vibration and white noise tests.
(5) In general, the instantaneous natural frequencies at the beginning of each earthquake are closer to the corresponding natural frequencies identified based on the ambient vibration test data performed before the earthquake while the instantaneous natural frequencies at the end of each earthquake are closer to those identified based on white noise test data performed after the earthquake.

This study highlights the effectiveness of the DSI method for short-time (instantaneous) modal identification of nonlinear structural systems. It is expected that accurate estimates of instantaneous modal parameters to be used for characterizing the hysteretic behavior of structural components (e.g., substructures), which is the topic of an ongoing research by the authors. This can be done through computing the tangent stiffness (corresponding to stiffness of the linearized system at considered time instant) of different structural components based on the identified instantaneous modal parameters. The predicted hysteretic material behavior provides information for realistic and comprehensive damage measures accounting for nonlinear behavior such as material yielding, loss of stiffness, and strength degradation which are common sources of “structural damage”. In addition, the instantaneous mode

shapes identified using DSI for nonlinear structural systems at different levels of input energy can provide an estimate for the nonlinear normal modes of the structural system.

ACKNOWLEDGEMENTS

The authors would like to thank Professors Joel Conte and Jose Restrepo at University of California San Diego for making the shake table test data available for this study. Assistance of Professors Marios Panagiotou and Ozgur Ozcelik as well as the technical staff at the Englekirk Structural Engineering Center in collecting the test data used in this study is also greatly acknowledged.

REFERENCE

[1] G. Kerschen, K. Worden, A.F. Vakakis, J.C. Golinvala, Past, present and future of nonlinear system identification in structural dynamics, Mechanical Systems and Signal Processing 20 (3) (2006) 505-592.

[2] S.K. Kunnath, J.B. Mander, L. Fang, Parameter identification for degrading and pinched hysteretic structural concrete systems, Engineering Structures 19 (3) (1997) 224-232.

[3] N. Ajavakom, C.H. Ng, F. Ma, Performance of nonlinear degrading structures: Identification, validation, and prediction, Computers and Structures 86 (7-8) (2008) 652-662.

[4] M. Nayyerloo, J.G. Chase, G.A. MacRae, X.Q. Chen, LMS-based approach to structural health monitoring of nonlinear hysteretic structures, Structural Health Monitoring (2011) in press, doi: 10.1177/1475921710379519.

[5] V.K. Gupta, S.R.K. Nielsen, P.H. Kirkegaard, A preliminary prediction of seismic damage-based degradation in RC structures, Earthquake Engineering and Structural Dynamics 30 (7) (2001) 981-993.

[6] R. Ceravolo, G.V. Demarie, S. Erlicher, Instantaneous identification of degrading hysteretic oscillators under earthquake excitation, Structural Health Monitoring 9 (5) (2010) 447-464.

[7] M. Wu, A.W. Smyth, Application of the unscented Kalman filter for real-time nonlinear structural system identification, Structural Control and Health Monitoring 14 (7) (2007) 971-990.

[8] E.N. Chatzi, A.W. Smyth, S.F. Masri, Experimental application of on-line parametric identification for nonlinear hysteretic systems with model uncertainty, Structural Safety 32 (5) (2010) 326-337.

[9] H. Zhang, G.C. Foliente, Y. Yang, F. Ma, Parameter identification of inelastic structures under dynamic loads, Earthquake Engineering and Structural Dynamics 31 (5) (2002) 1113-1130.

[10] S.W. Shaw, C. Pierre, Non-linear normal modes and invariant manifolds, Journal of Sound and Vibration 150 (1) (1991) 170-173.

[11] A.F. Vakakis, Non-linear normal modes and their applications in vibration theory: an overview, Mechanical Systems and Signal Processing 11 (1) (1997) 3-22.

[12] G. Kerschen, M. Peeters, J.C. Golinval, A.F. Vakakis, Nonlinear normal modes, Part I: A useful framework for the structural dynamicist, Mechanical Systems and Signal Processing 23 (1) (2009) 170-94.

[13] S.W. Doebling, C.R. Farrar, M.B. Prime, A summary review of vibration-based damage identification methods, The Shock and Vibration Digest 30 (2) (1998) 91-105.

[14] H. Sohn, C.R. Farrar, F.M. Hemez, D.D. Shunk, D.W Stinemates, B.R. Nadler, A review of structural health monitoring literature: 1996-2001. Los Alamos National Laboratory Report, LA-13976-MS, Los Alamos, New Mexico, USA, 2003.

[15] M. Phan, L.G. Horta, J.N. Juang, R.W. Longman, Identification of linear systems by an asymptotically stable observer, NASA Technical Paper No. TP-3164, Langley Research Center, Hampton, VA, 1992.

[16] L. Ljung, System identification: Theory for the user, second ed., Prentice-Hall, Englewood Cliffs, N.J, 1999.

[17] H. Lus, R. Betti, R.W. Longman, Obtaining refined first order predictive models of linear structural systems, Earthquake Engineering and Structural Dynamics 31 (7) (2002) 1413-1440.

[18] C.R. Farrar, G.H. III. James, System identification from ambient vibration measurements on a bridge, Journal of Sound and Vibration 205 (1) (1997) 1-18.

[19] R. Brincker, C. Ventura, P. Andersen, Damping estimation by frequency domain decomposition, in: Proceedings of the International Conference on Modal Analysis (IMAC-XIX), 2001.

[20] J.M. Caicedo, S.J. Dyke, E.A. Johnson, Natural excitation technique and eigensystem realization algorithm for Phase I of the IASC-ASCE benchmark problem: simulated data, Journal of Engineering Mechanics, ASCE 130 (1) (2004) 49-61.

[21] F. Magalhaes, A. Cunha, E. Caetano, R. Brincker, Damping estimation using free decays and ambient vibration tests, Mechanical Systems and Signal Processing 24 (5) (2009) 1274–1290.

[22] E. Reynders, D. Degrauwe, G. De Roeck, F. Magalhaes, E. Caetano, Combined experimental-operational modal testing of footbridges, Journal of Engineering Mechanics 136 (6) (2010) 687-696.

[23] P. Van Overschee, B. De Moore, Subspace identification for linear systems, Kluwer Academic Publishers, Norwell, MA, USA, 1996.

[24] B. Peeters, G. De Roeck, Reference-based Stochastic Subspace Identification for Output-Only Modal Analysis, Mechanical Systems and Signal Processing 13(6) (1999) 855-878.

[25] B. Moaveni, A.R. Barbosa, J.P. Conte, F.M. Hemez, Uncertainty analysis of modal parameters obtained from three system identification methods, in: Proceedings of International Conference on Modal Analysis (IMAC-XXV), Orlando, FL, 2007.

[26] B. Moaveni, X. He, J.P. Conte, J.I. Restrepo, M. Panagiotou, System identification study of a seven-story full-scale building slice tested on the UCSD-NEES shake table, Journal of Structural Engineering 137 (6) (2011) 705-717.

[27] X. He, B. Moaveni, J.P. Conte, A. Elgamal, S.F. Masri, System identification of Alfred Zampa Memorial Bridge using dynamic field test data, Journal of Structural Engineering 135 (1) (2009) 54-66.

[28] M. Ruzzene, A. Fasana, L. Garibaldi, B. Piombo, Natural frequencies and dampings identification using wavelet transform: application to real data, Mechanical Systems and Signal Processing 11 (2) (1997) 207-218.

[29] W.J. Staszewski, Identification of damping in MDOF systems using time-scale decomposition, Journal of Sound and Vibration 203 (2) (1997) 283-305.

[30] A. Kareem, T. Kijewski, Time-frequency analysis of wind effects on structures, Journal of Wind Engineering and Industrial Aerodynamics 90 (12-5) (2002) 1435-1452.

[31] T. Kijewski, A. Kareem, On the presence of end effects and their melioration in wavelet-based analysis, Journal of Sound and Vibration 256 (5) (2002) 980-988.

[32] T. Kijewski, A. Kareem, Wavelet transforms for system identification in civil engineering, Computer-Aided Civil and Infrastructure Engineering 18 (5) (2003) 339-355.

[33] B.F. Yan, A. Miyamoto, E. Brühwiler, Wavelet transform based modal parameter identification considering uncertainty, Journal of Sound and Vibration 291 (1-2) (2005) 285-301.

[34] B. Yan, A. Miyamoto, A comparative study of modal parameter identification based on wavelet and Hilbert-Huang transforms, Computer-aided Civil and Infrastructure Engineering 21 (1) (2006) 9-23.

[35] P.D. Spanos, A. Giaralis, N.P. Politis, J.M. Roesset, Numerical treatment of seismic accelerograms and of inelastic seismic structural responses using harmonic wavelets, Computer-Aided Civil and infrastructure Engineering 22 (4) (2007) 254-264.

[36] M. Feldman, Nonlinear system vibration analysis using the Hilbert transform - I. Free vibration analysis method „FREEVIB", Mechanical Systems and Signal Processing 8 (2) (1994) 119-127.

[37] M. Feldman, Nonlinear system vibration analysis using the Hilbert transform - II. Forced vibration analysis method „FORCEVIB", Mechanical Systems and Signal Processing 8 (3) (1994) 309-318.

[38] M. Feldman, Non-linear free vibration identification via the Hilbert transform, Journal of Sound and Vibration 208 (3) (1997) 475-489.

[39] O. Gottlieb, M. Feldman, S.C.S. Yim, Parameter identification of nonlinear ocean mooring systems using the Hilbert transform, Journal of Offshore Mechanics and Arctic Engineering 118 (1) (1996) 29-36.

[40] N.E. Huang, Z. Shen, S.R. Long, M.C. Wu, H.H. Shih, Q. Zheng, N.C. Yen, C.C. Tung, H.H. Liu, The empirical mode decomposition and the Hilbert spectrum for nonlinear and non-stationary time series analysis, Proc. of the Royal Society of London Series A - Mathematical, Physical and Engineering Sciences 454 (1971) (1998) 903-995.

[41] J.N. Yang, Y. Lei, S.W. Pan, N. Huang, System identification of linear structures based on Hilbert-Huang spectral analysis; Part 1: Normal modes, Earthquake Engineering and Structural Dynamics 32 (9) (2003) 1443-1467.

[42] J.N. Yang, Y. Lei, S.W. Pan, N. Huang, System identification of linear structures based on Hilbert-Huang spectral analysis; Part 2: Complex modes, Earthquake Engineering and Structural Dynamics 32 (10) (2003) 1533-1554.

[43] J.N. Yang, S. Lin, Hilbert-Huang based approach for structural damage detection, Journal of Engineering Mechanics 130 (1) (2004) 85-95.

[44] T.K. Hasselman, M.C. Anderson, W.G. Gan, Principal component analysis for nonlinear model correlation, in: Proceedings of the 16th International Modal Analysis Conference (IMAC XVI), Santa Barbara, 1998.

[45] F.M. Hemez, S.W. Doebling, Review and assessment of model updating for non-linear transient dynamics, Mechanical Systems and Signal Processing 15 (1) (2001) 45-74.

[46] V. Lenaerts, G. Kerschen, J.C. Golinval, Proper orthogonal decomposition for model updating of non-linear mechanical systems, Mechanical Systems and Signal Processing 15 (1) (2001) 31-43.

[47] V. Lenaerts, G. Kerschen, J.C. Golinval, Identification of a continuous structure with a geometrical non-linearity - part II: proper orthogonal decomposition, Journal of Sound and Vibration 262 (4) (2003) 907-919.

[48] C.S. Huang, S.L. Hung, W.C. Su, C.L. Wu, Identification of time-variant modal parameters using time-varying autoregressive with exogenous input and low-order polynomial function, Computer-Aided Civil and Infrastructure Engineering 24 (2009) 470–491.

[49] C.H. Loh, C.Y. Lin, C.C. Huang, Time domain identification of frames under earthquake loadings, Journal of Engineering Mechanics - ASCE, 126 (7) (2000) 693–703.

[50] Y. Grenier, Time-dependent ARMA modeling of nonstationary signals, IEEE Transactions on Acoustics, Speech, and Signal Processing, 31 (1983) 899–911.

[51] A.G. Poulimenos, S.D. Fassois, Parametric time-domain methods for non-stationary random vibration modelling and analysis - a critical survey and comparison, Mechanical Systems and Signal Processing, 20 (2006) 763–816.

[52] A.G. Poulimenos, S.D. Fassois, Output-only stochastic identification of a time-varying structure via functional series TARMA models, Mechanical Systems and Signal Processing, 23 (4) (2009) 1180–1204.

[53] S. Mazzoni, M.H. Scott, F. McKenna, G.L. Fenves, et al., Open System for Earthquake Engineering Simulation - user manual (version 1.7.3), Pacific Earthquake Engineering Research Center, University of California, Berkeley, California, 2006.

[54] A. Saltelli, K. Chan, E.M. Scott, Sensitivity Analysis, John Wiley & Sons, New York, 2000.

[55] M. Panagiotou, J.I. Restrepo, J.P. Conte, Shake-table test of a full-scale 7-story building slice - Phase I: Rectangular wall, Journal of Structural Engineering 137 (6) (2011) 691-704.

[56] F. Ma, H. Zhang, A. Bockstedte, G.C. Foliente, P. Paevere, Parameter analysis of the differential model of hysteresis, Journal of Applied Mechanics 71 (3) (2004) 342-349.

[57] B. Moaveni, A. Stavridis, G. Lombaert, J.P. Conte, P.B. Shing, Finite element model updating for assessment of progressive damage in a three-story infilled RC frame, Journal of Structural Engineering, ASCE (2012) in press.

TABLES

Table 1. Description of input factor and their considered levels

Factor	Description	Levels
M	Type of material nonlinearity	2 levels (bilinear, Giuffré-Menegotto-Pinto)
R	Level of nonlinearity	2 levels (R = 4, 6)
I	Input excitation	2 levels (Northridge, Imperial Valley)
L	Length of identification windows	2 levels (1, 2 seconds)

Table 2. Natural frequencies and damping ratios of the underlying linear 7-DOF systems

	Mode 1	Mode 2	Mode 3	Mode 4	Mode 5	Mode 6	Mode 7
Natural Frequency [Hz]	2.00	4.95	7.68	11.38	14.73	17.32	18.94
Damping ratio [%]	2.0	1.5	1.7	2.1	2.7	3.1	3.3

Table 3. Mean/maximum estimation errors [Hz] of the identified natural frequencies for SDOF systems

	I = Northridge				I = Imperial Valley			
	M = bilinear		M = Pinto		M = bilinear		M = Pinto	
	R=4	R=6	R=4	R=6	R=4	R=6	R=4	R=6
DSI (L = 1)	0.08/0.49	0.15/0.76	0.09/0.31	0.10/0.36	0.05/0.19	0.10/0.40	0.05/0.15	0.07/0.19
DSI (L = 2)	0.09/0.30	0.09/0.38	0.05/0.20	0.11/0.21	0.08/0.38	0.16/0.55	0.05/0.15	0.07/0.16
WT	0.12/0.28	0.17/0.37	0.13/0.35	0.29/1.18	0.26/0.64	0.28/0.66	0.22/0.64	0.23/0.64

Table 4. Mean/maximum estimation errors [Hz] of the identified natural frequencies for 7-DOF systems

		I = Northridge				I = Imperial Valley			
		M = bilinear		M = Pinto		M = bilinear		M = Pinto	
		R=4	R=6	R=4	R=6	R=4	R=6	R=4	R=6
Mode 1	DSI (L = 1)	0.08/0.27	0.08/0.25	0.09/0.24	0.07/0.22	0.07/0.30	0.07/0.22	0.03/0.13	0.04/0.13
	DSI (L = 2)	0.05/0.15	0.06/0.14	0.03/0.11	0.04/0.14	0.05/0.15	0.08/0.17	0.02/0.05	0.03/0.07
	WT	0.15/0.28	0.15/0.32	0.14/0.28	0.13/0.29	0.21/0.75	0.21/0.75	0.20/0.75	0.20/0.75
Mode 2	DSI (L = 1)	0.07/0.15	0.08/0.33	0.06/0.17	0.08/0.25	0.07/0.45	0.09/0.33	0.09/0.35	0.11/0.28
	DSI (L = 2)	0.05/0.16	0.08/0.19	0.03/0.11	0.08/0.15	0.09/0.28	0.11/0.37	0.08/0.22	0.08/0.20
Mode 3	DSI (L = 1)	0.09/0.41	0.16/0.64	0.12/0.46	0.20/0.60	0.08/0.47	0.13/0.40	0.06/0.29	0.04/0.44
	DSI (L = 2)	0.09/0.54	0.17/0.60	0.10/0.55	0.15/0.36	0.09/0.57	0.08/0.27	0.04/0.21	0.04/0.35

Table 5. Standard deviation of the mean and maximum estimation errors [Hz] for SDOF and 7-DOF systems

	SDOF	7-DOF Mode 1	7-DOF Mode 2	7-DOF Mode 3
Mean estimation error	0.03	0.02	0.02	0.05
Maximum estimation error	0.17	0.07	0.10	0.13

Table 6. Natural frequency [Hz] of the first mode identified based on low-amplitude ambient vibration and 0.03 g RMS white noise base excitation test data before and after each earthquake

	After EQ1	After EQ2	After EQ3	Before EQ4*	After EQ4
Ambient vibration	1.86	1.67	1.46	1.58	1.02
0.03 g RMS white noise	1.51	1.25	1.13	1.20	0.85

* Between EQ3 and EQ4, the test structure was slightly reinforced

Figure

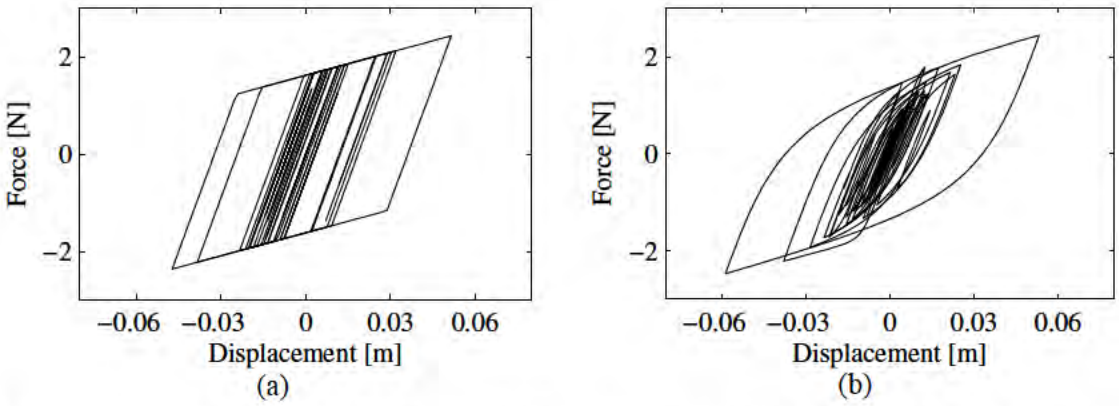

Figure 1. Hysteretic response of nonlinear SDOF systems (R = 4) to the Northridge earthquake record with (a) bilinear, and (b) Giuffré-Menegotto-Pinto material models

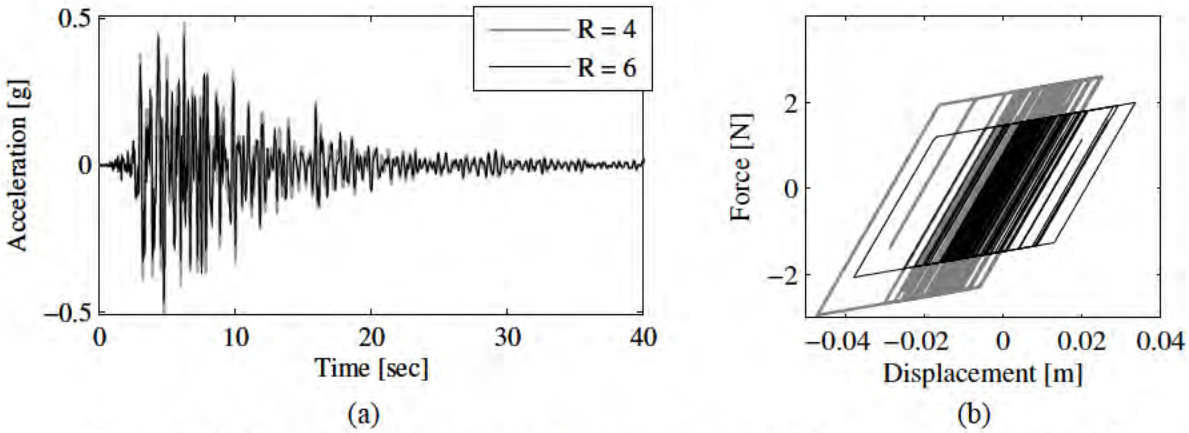

(a) (b)

Figure 2. (a) Relative acceleration time histories of two SDOF systems with R = 4 and R = 6, respectively, and Giuffré-Menegotto-Pinto material models subjected to the Northridge earthquake, and (b) force-displacement hysteretic plot of two SDOF systems with R = 4 and R = 6, respectively, and bilinear material models subjected to the Imperial Valley earthquake

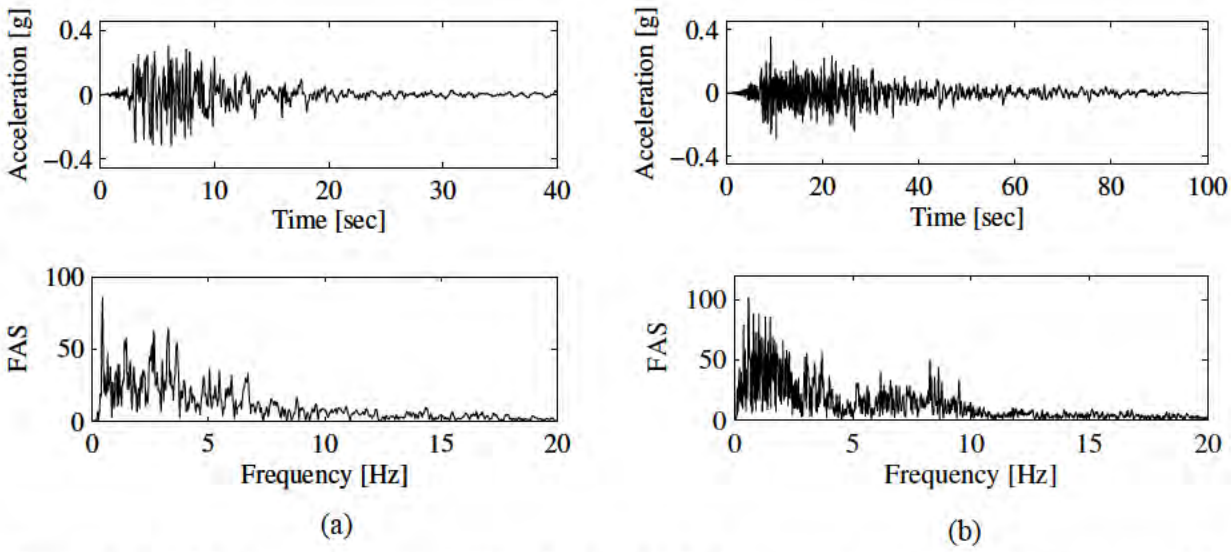

Figure 3. Acceleration time history and Fourier Amplitude Spectra of (a) longitudinal component of the 1994 Northridge earthquake recorded at the Oxnard Boulevard station in Woodland Hills, and (b) longitudinal component of the 1979 Imperial Valley earthquake recorded at the Delta station

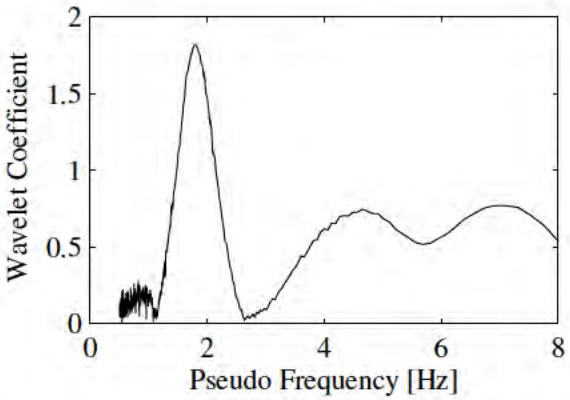

Figure 4. Wavelet spectrum of the response of a nonlinear SDOF system (bilinear and R = 6) subjected to Northridge earthquake at t = 17 second

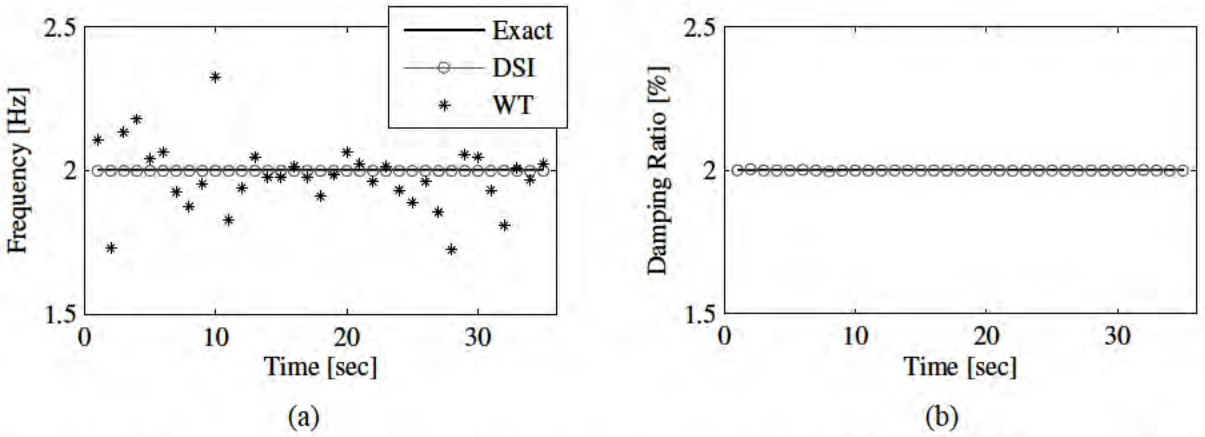

(a) (b)

Figure 5. (a) Instantaneous natural frequencies, and (b) damping ratios of a linear SDOF system identified using the WT and DSI based on its response to Northridge earthquake

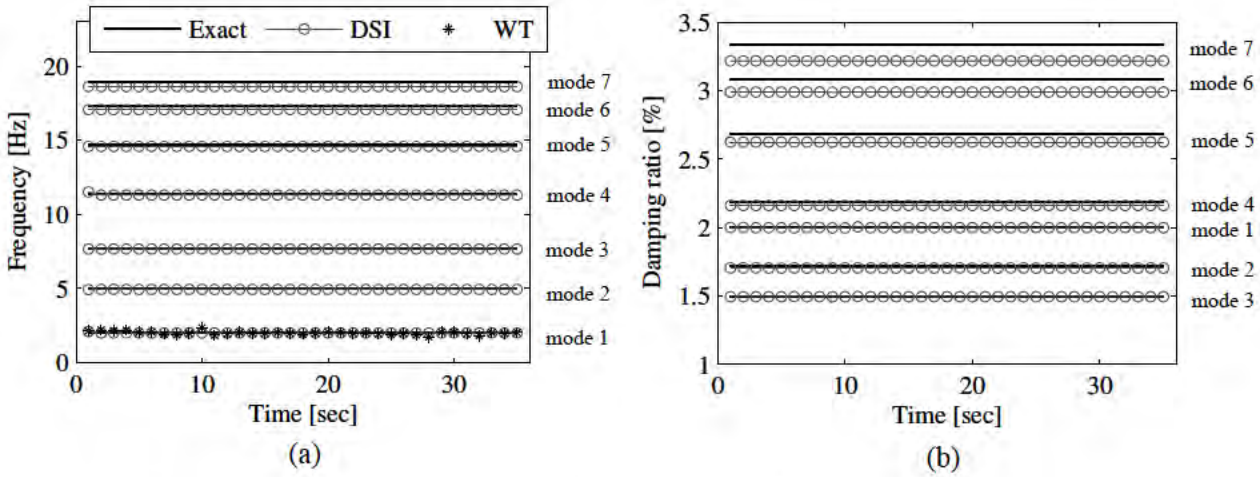

Figure 6. (a) Instantaneous natural frequencies, and (b) damping ratios of a linear 7-DOF system identified using the WT and DSI based on its response to Northridge earthquake

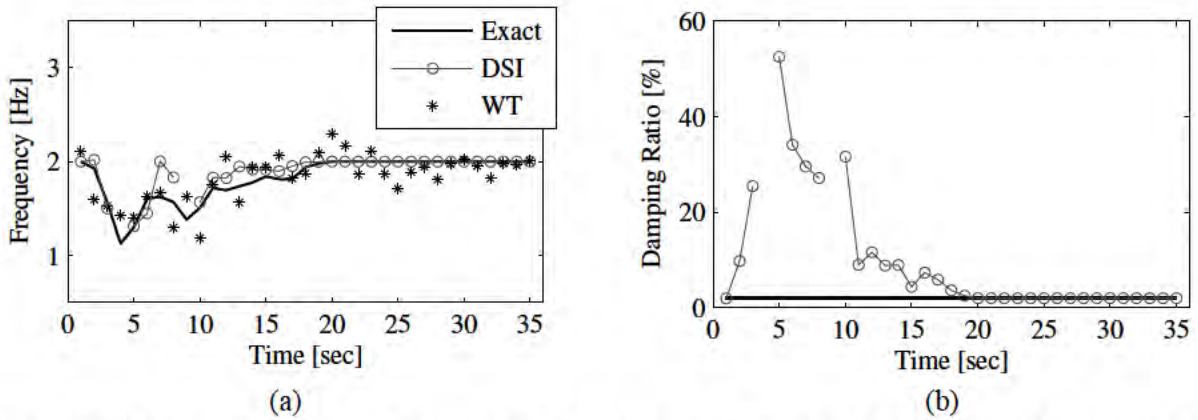

(a) (b)

Figure 7. (a) Instantaneous natural frequencies, and (b) damping ratios of a nonlinear SDOF system with M = bilinear, R = 6, I = Northridge, and L = 2, identified using DSI and WT

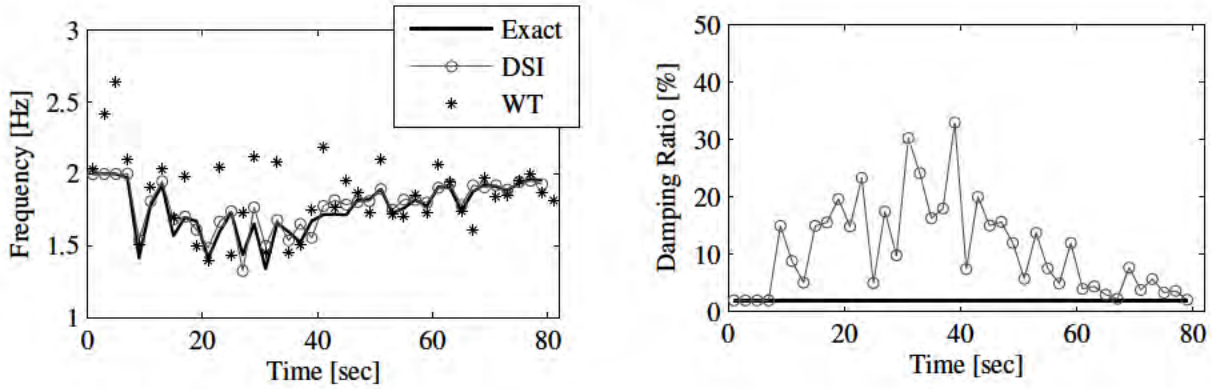

(a) (b)

Figure 8. (a) Instantaneous natural frequencies, and (b) damping ratios of a nonlinear SDOF system with M = Pinto, R = 6, I = Imperial Valley, and L = 1, identified using DSI and WT

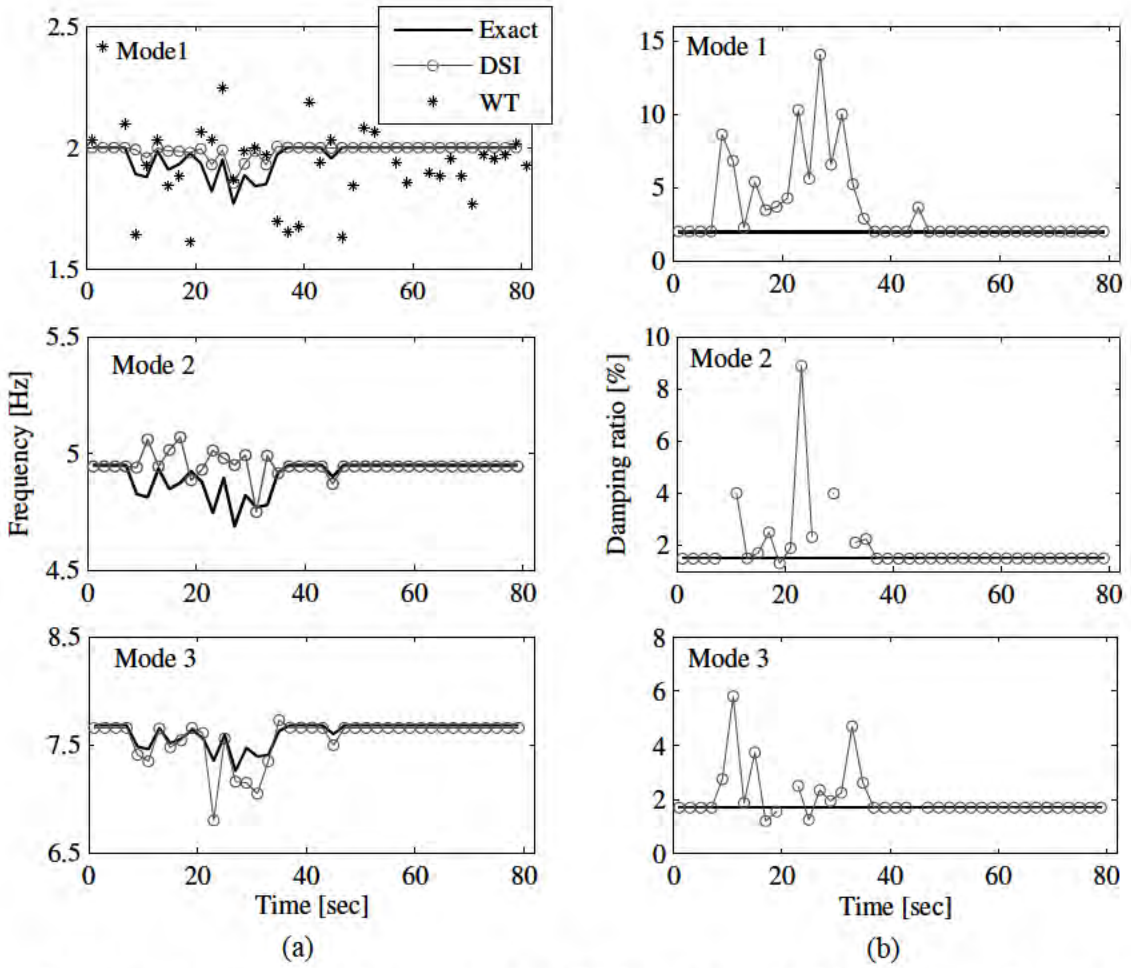

Figure 9. (a) Instantaneous natural frequencies, and (b) damping ratios of the first three vibration modes of a nonlinear 7-DOF system with M = bilinear, R = 4, I = Imperial Valley, and L = 2, identified using DSI and WT (for the first mode only)

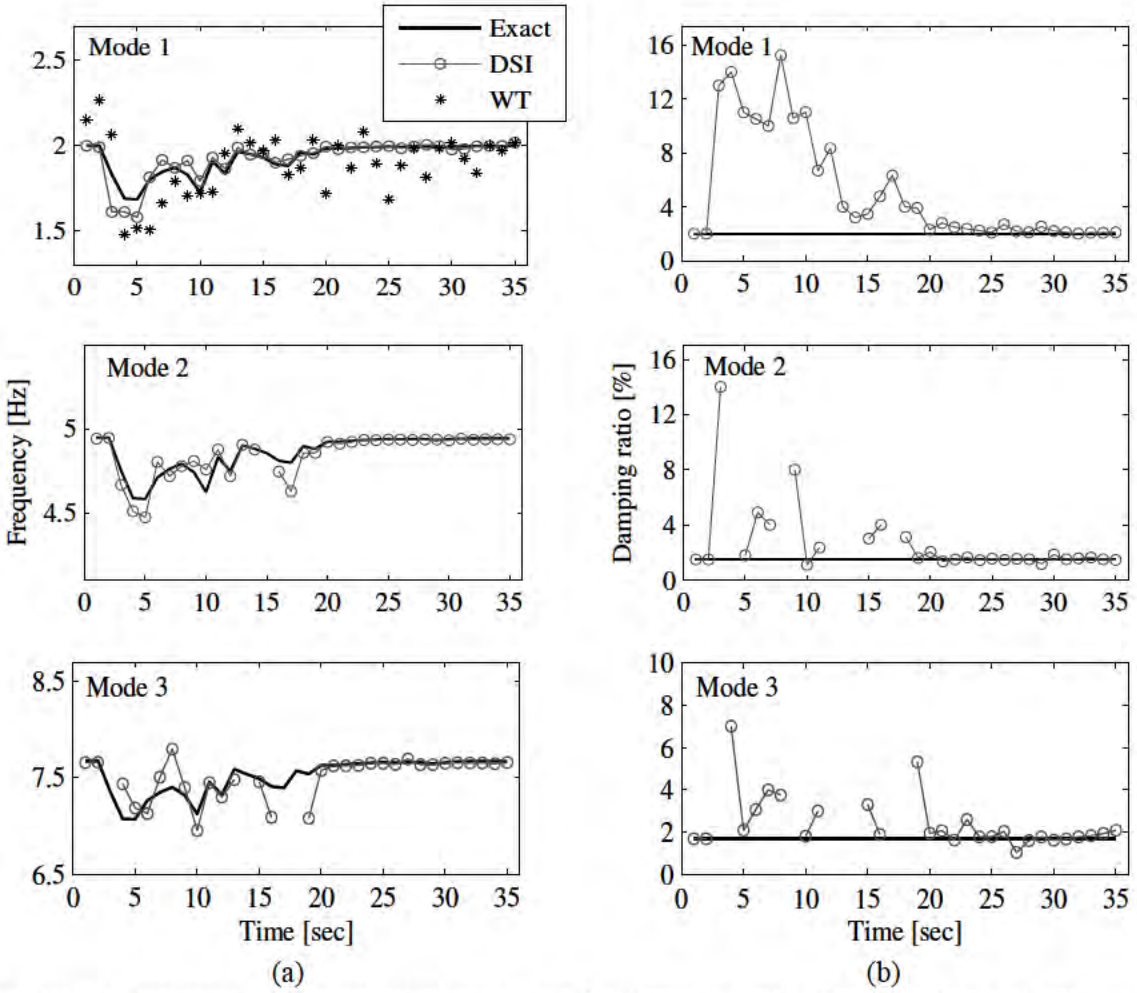

Figure 10. (a) Instantaneous natural frequencies, and (b) damping ratios of the first three vibration modes of a nonlinear 7-DOF system with M = Pinto, R = 4, I = Northridge, and L = 1, identified using DSI and WT (for the first mode only)

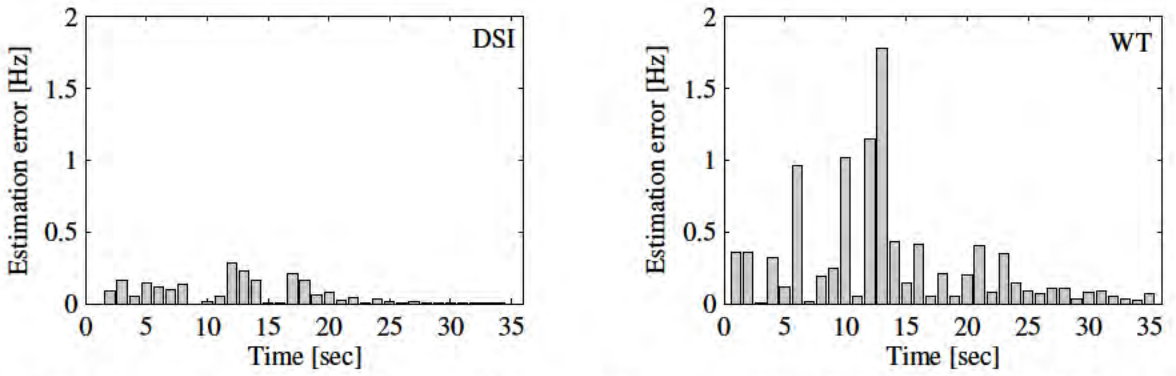

Figure 11. Estimation error time history of the natural frequencies identified using DSI and WT methods for a SDOF system with M = Pinto, R = 6, I = Northridge, L = 2

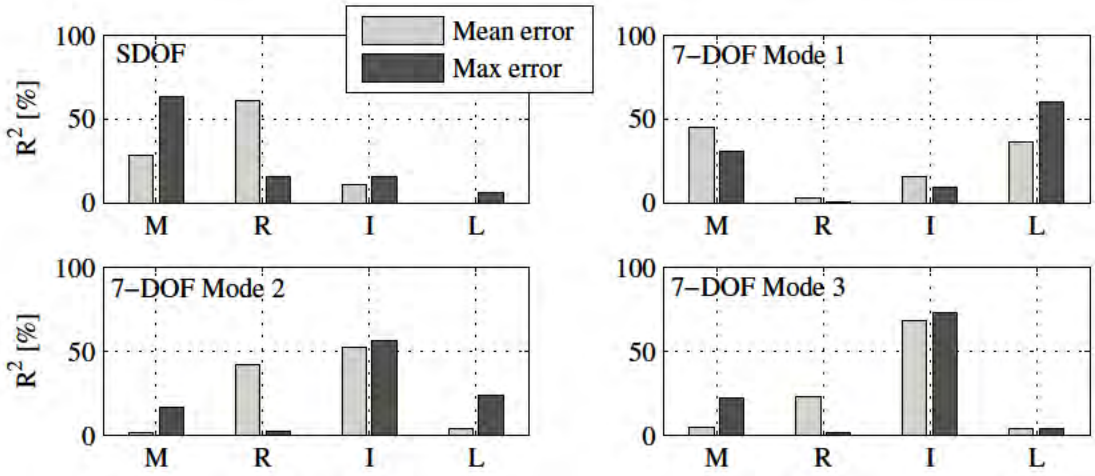

Figure 12. Coefficient-of-determination (R^2) of the mean and maximum estimation errors for the four input factors and the SDOF and 7-DOF systems

Figure 13. Full-scale shear wall test structure

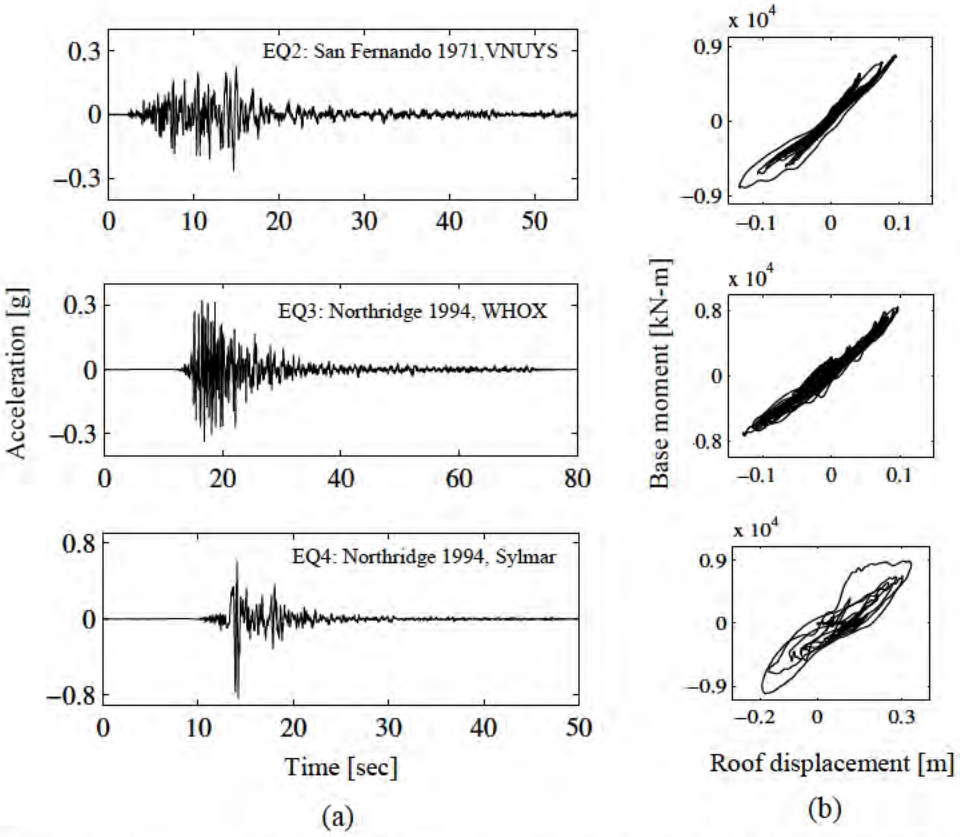

Figure 14. (a) Acceleration time histories of the three considered earthquakes measured on shake table, and (b) base moment versus roof displacement of the structure during the three seismic base excitations

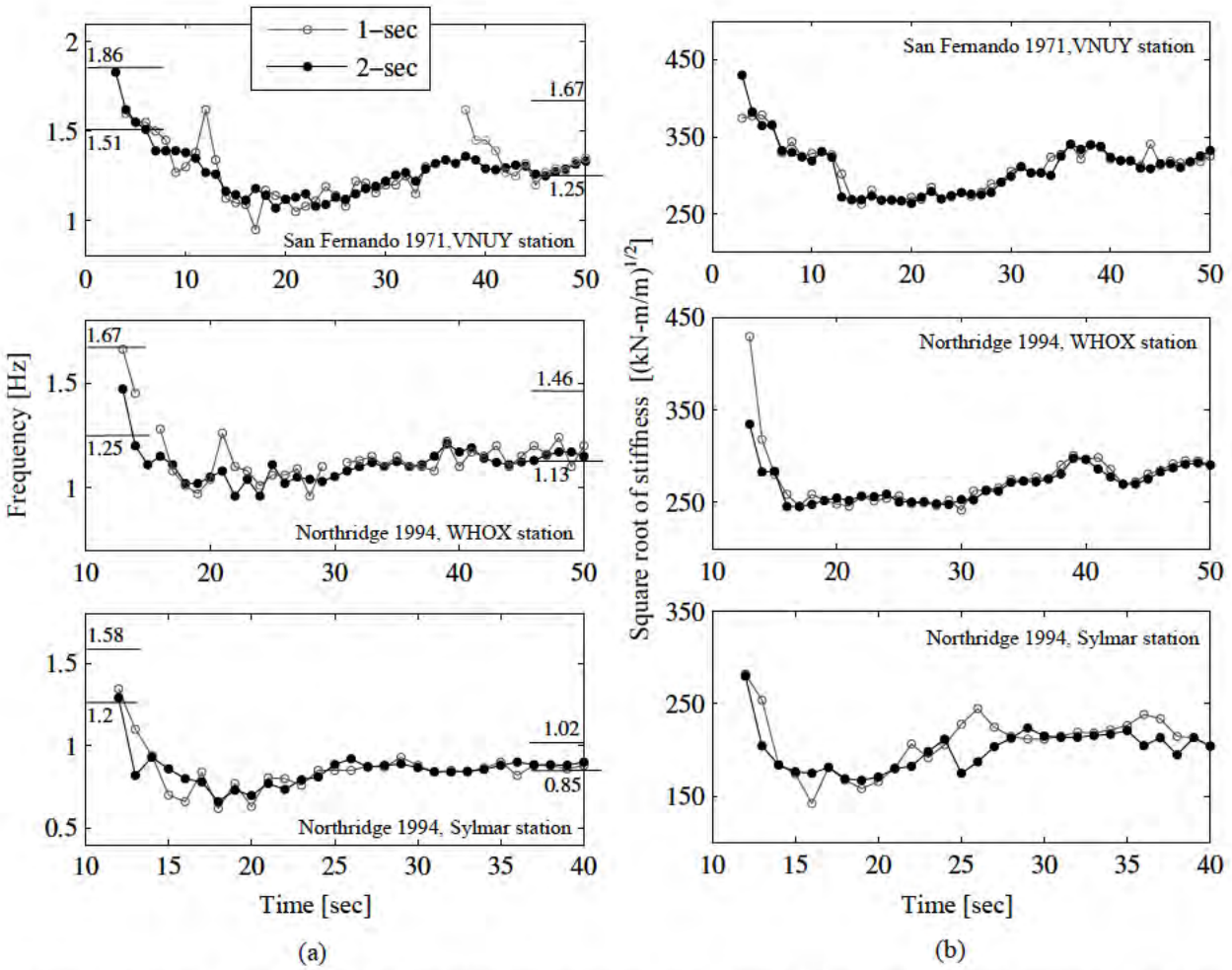

Figure 15. Time histories of (a) instantaneous fundamental natural frequency, and (b) square root of an effective global stiffness measure of the test structure, estimated using 1- or 2-second data windows during the three considered earthquakes